

# pMixFed: Efficient Personalized Federated Learning through Adaptive Layer-Wise Mixup

Yasaman Saadati<sup>1,2</sup>, Mohammad Rostami<sup>3</sup>, and M. Hadi Amini<sup>1,2</sup>

<sup>1</sup> Knight Foundation School of Computing and Information Sciences, Florida International University

<sup>2</sup> Sustainability, Optimization, and Learning for InterDependent networks laboratory (solid lab)

<sup>3</sup> University of Southern California

ysaadati@fiu.edu, rostamim@usc.edu, moamini@fiu.edu

## Abstract

Traditional Federated Learning (FL) methods encounter significant challenges when dealing with heterogeneous data and providing personalized solutions for non-IID scenarios. Personalized Federated Learning (PFL) approaches aim to address these issues by balancing generalization and personalization, often through parameter decoupling or partial models that freeze some neural network layers for personalization while aggregating other layers globally. However, existing methods still face challenges of global-local model discrepancy, client drift, and catastrophic forgetting, which degrade model accuracy. To overcome these limitations, we propose **pMixFed**, a dynamic, layer-wise PFL approach that integrates mixup between shared global and personalized local models. Our method introduces an adaptive strategy for partitioning between personalized and shared layers, a gradual transition of personalization degree to enhance local client adaptation, improved generalization across clients, and a novel aggregation mechanism to mitigate catastrophic forgetting. Extensive experiments demonstrate that pMixFed outperforms state-of-the-art PFL methods, showing faster model training, increased robustness, and improved handling of data heterogeneity under different heterogeneous settings. Our code is available for reproducing our results: <https://github.com/YasMinSdt/pMixFed>.

## 1. Introduction

The goal in federated learning (FL) [22] is to facilitate collaborative learning of several machine learning (ML) models in a decentralized scheme. FL requires addressing data privacy, catastrophic forgetting, and client drift problem<sup>1</sup> [15, 31, 36, 38, 43]. Existing FL methods cannot ad-

<sup>1</sup> A phenomenon where the global model fails to serve as an accurate representation because local models gradually drift apart due to high data

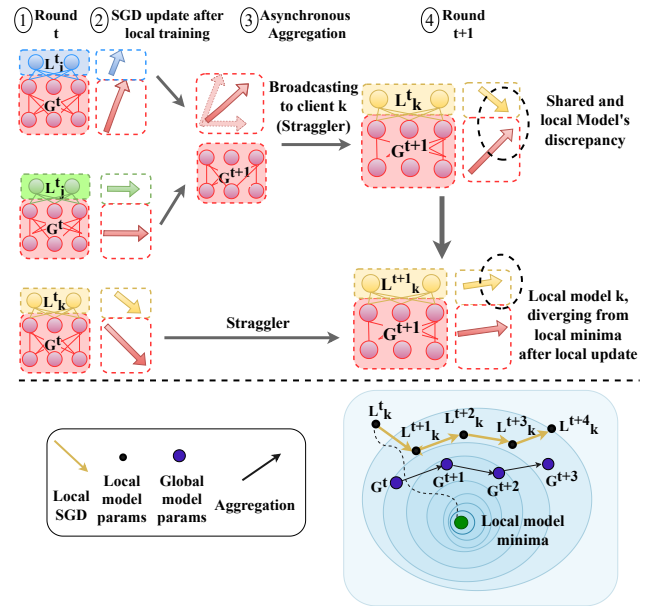


Figure 1. Discrepancy between personalized and global shared layers in Partial PFL: (1) The global model,  $G^t$ , is constructed by aggregating asynchronous local updates from clients, denoted as  $L_i^t$ ,  $L_j^t$ , and  $L_k^t$ . (2),(3) In communication round  $t$ , available clients  $i$  and  $j$  aggregate shared parameters to produce the updated global model  $G^{t+1}$ , while the personalized parameters, such as  $L_k^t$ , remain unchanged for unavailable clients. (4) This integration of distinct models,  $G^{t+1}$  and  $L_k^t$ , induces inconsistencies in the overall model updates. (Bottom) During the joint training of generalized and personalized models, the gradient updates from the generalized layers are impacted by the gradients from personalized layers, resulting in catastrophic forgetting, performance drop and slower convergence rates.

dress all these challenges with non-IID (non-Independent and Identically Distributed) data. For instance, although “FedAvg” [32] demonstrates strong generalization performance, it fails to provide personalized solutions for a cohort of clients with non-IID datasets. Hence, the global model, or one “average client” in “FedAvg”, may not adequately heterogeneity.

represent all individual local models in non-IID settings due to client-drift [53]. Personalized FL (PFL) methods handle data heterogeneity by considering both generalization and personalization during the training stage. Since there is a trade-off between generalization and personalization in heterogeneous environments, PFL methods leverage heterogeneity and diversity as advantages rather than adversities [35, 47]. A group of PFL approaches train personalized local models on each device while collaborating toward a shared global model. Partial PFL, also known as parameter decoupling, involves using a partial model sharing, where only a subset of the model is shared while other parameters remain “frozen” to balance generalization and personalization until the subsequent round of local training.

While partial PFL methods are effective in mitigating catastrophic forgetting, strengthening privacy, and reducing computation and communication overhead [34, 45], there are still some unaddressed challenges. First, the question of *when, where, and how to optimally partition the full model?* remains unresolved. Recent studies [34, 45] have shown that there is no “one-size-fits-all” solution; the best or optimal partitioning strategy depends on factors such as task type (e.g., next word prediction or speech recognition) and local model architecture. An improper partitioning choice can lead to issues such as underfitting, overfitting, increased bias, and catastrophic forgetting. Some studies [29] suggest that personalized layers should reside in the base layers, while others [4, 9] argue that the base layers contain more generalized information and should be shared. Further, the use of a fixed partitioning strategy across all communication rounds for heterogeneous clients can limit the efficacy of collaborative learning. For instance, if the performance of the client suddenly drops due to new incoming data, the partitioning strategy should be changed because the client requires more frozen layers. Another issue is catastrophic forgetting of the previously shared global knowledge after only a few rounds of local training because the shared global model can be completely overwritten by local updates leading to generalization degradation [15, 31, 41, 54]. Most importantly, partial models may experience slower convergence compared to full model personalization, as frozen local model updates can diverge in an opposite direction from the globally-shared model. Since the generalized and personalized models are trained on non-IID datasets, there might also be a domain shift, leading to model discrepancy as depicted in Figure 1. These discrepancies arise from variations in local and global objective functions, differences in initialization, and asynchronous updates [24, 56]. As a result, merging the shared and the personalized layers can disrupt information flow within the network, impede the learning process, and lead to a slower convergence rate or accuracy drop in partial PFL models such as FedAlt and FedSim

[34]<sup>2</sup>. Further, while partial PFL techniques contribute to an overall improved training accuracy, they can reduce the test accuracy on some devices, particularly in devices with limited samples, leading to variations in results in terms of the performance level [34]. Hence, there is a need for novel solutions to achieve the following goals in PFL:

- **Dynamic and Adaptive Partitioning:** The balance between shared and personalized layers should be dynamically and adaptively adjusted for each client during every communication round, rather than relying on a static, fixed partitioning strategy for all participants.
- **Gradual Personalization Transition:** The degree of personalization should transition gradually across layers, as opposed to an “all-or-nothing” approach that employs strict partitioning or hard splits within the model discussed in Figure 1. This ability allows nuanced adaptation for individual client needs due to heterogeneity.
- **Improved Generalization Across All Clients:** The average personalization accuracy should be such that the global model is unbiased toward specific subsets of clients.
- **Mitigation of Catastrophic Forgetting:** The strategy should address the catastrophic forgetting problem by incorporating mechanisms to strengthen the generalization and retain the state of the previous global model when updating the global model in aggregation.
- **Scalability and Adaptability:** The approach should be fast, scalable, and easily adaptable to new cold-start clients while accounting for model/device heterogeneity.

To achieve the above, we propose “pMixFed”, a layer-wise, dynamic PFL approach that integrates Mixup [61] between the shared global and personalized local models’ layers during both the broadcasting (global model sharing with local clients) and aggregation (aggregating distributed local models to update the global model) stages within a partial PFL framework. Our main contributions include:

- We develop an online, dynamic interpolation method between local and global models using Mixup [57], effectively addressing data heterogeneity and scalable across varying cohort sizes, degrees of data heterogeneity, and diverse model sizes and architectures.
- Our solutions facilitate a gradual increase in the degree of personalization across layers, rather than relying on a strict cut-off layer, helping to mitigate client drift.
- We introduce a new fast and efficient aggregation technique which addresses catastrophic forgetting by keeping the previous global model state.
- “pMixFed” reduces the participant gap (test accuracy for cold-start users) and the out-of-sample gap (test accuracy on unseen data) caused by data heterogeneity through linear interpolation between client updates, thereby mitigating the impact of client drift.

<sup>2</sup>More details on this is discussed in section 5.3.

## 2. Related Work

PFL aims to adapt local models to the individual needs, preferences, and contexts of each participant. Since the inception of FL, various PFL approaches have been explored to address the challenges stemming from heterogeneity, categorized into three areas: 1) data-centric strategies 2) global model adaptation, and 3) local model personalization. The following provide a more detailed discussion of these three approaches:

**Data-centric:** These approaches in PFL aim to address data heterogeneity and class imbalances by manipulating statistical data properties, such as data size, distribution, and local data selection [47]. Examples of these techniques include data normalization, feature engineering, data augmentation, synthetic data generation, and client selection. Representative methods, such as Astraea [11], P2P k-SMOTE [50], FedMCCS [1], FedAug [19], [63], and FedHome [52], exemplify data-centric approaches. The shortcoming of these methods is that they often modify the natural distribution and statistical characteristics of federated data, potentially injecting bias or eliminating valuable, rare information. Additionally, many of these strategies depend on the availability of proxy data on the global server, which may conflict with the privacy regulations of some entities.

**Global Model Adaptation:** In these approaches, a single global model is maintained on the server and subsequently adapted to individual local models in the following phase. The primary goals of these methods are: 1) learning a robust, generalized model and 2) enabling fast, efficient local model adaptation. Several techniques employ regularization terms to mitigate client drift and prevent model divergence during local updates e.g., FedProx [27], SCAF-FOLD [21], FL-MOON [26], and FedCurv [42]. Some of these approaches such as PerFedAvg [12], pFedMe [46], and pFedHN [39] leverage Meta-learning, and transfer learning e.g., FedStag [55], and DPFed [58], yet they introduce specific challenges. Meta-learning methods can be computationally intensive, while regularization techniques may add computational overhead by incorporating additional terms in the objective function. Similarly, transfer learning algorithms can be inefficient in terms of communication overhead and often require a public dataset to enhance the global model on the server. A common limitation across most adaptation techniques is the need for uniform model architecture across all clients, requiring devices with varying computational capabilities to use the same model size.

**Local Model Personalization:** The limitations of existing PFL methods have led to the development of local model personalization approaches that focus on training customized models for each client. Some approaches utilize multi-task learning (MTL), a collaborative framework that

facilitates information exchange across distinct tasks (e.g., FedRes [2], MOCHA [44], FedAMP [16], and Ditto [28]). Another category leverages knowledge distillation (KD) to support personalization when client-specific training objectives differ, as seen in FedDF [30], FedMD [25], FedGen [64], and FedGKT [14]. However, both MTL and KD can incur significant computational and communication overhead, limiting their scalability for large-scale FL deployments across resource-constrained devices.

**Partial PFL:** These methods, also known as parameter decoupling, are the primary focus of this paper. These methods mitigate catastrophic forgetting by retaining shared components while freezing other layers for personalization. FedPer [4] introduced partial models in FL, sharing only initial layers with generalized information and reserving final layers for personalization. FedBABU [33] divides the network into a shared body and a frozen head with fully connected layers. Other frameworks, such as FURL [6] and LG-FedAvg [29], apply partial PFL by retaining private feature embeddings or using compact representation learning for high-level features, respectively. Two baseline methods in this paper are FedAlt [43] and FedSim [34]. FedAlt uses a stateless FL paradigm, reconstructing local models from the global model, while FedSim synchronously updates shared and local models with each iteration.

**Limitations:** These methods face challenges such as model update discrepancies (as shown in Figure 1) and catastrophic forgetting, where shared layers may undergo significant changes after only a few rounds of local training, resulting in sudden accuracy drops. Additionally, users with high personalization accuracy may freeze more layers than cold-start users or unreliable participants, who should rely more heavily on the global model. These challenges have motivated our development of a dynamic, adaptive layer-wise approach to balance generalization and personalization across clients, allowing tuning at different communication rounds to accommodate varying performance conditions.

## 3. Problem Formulation

Consider  $K$  collaborating clients (or agents), each trying to optimize a local loss function  $F_k(\theta)$  on the distributed local dataset  $D_k = (x_k, y_k)$ , where  $(x, y)$  shows the data features and the corresponding labels, respectively. Since the agents collaborate, the parameters  $\theta$  (parameters of the global model) are shared across the agents. A basic FL objective function aims to optimize the overall global loss:

$$\min_{\theta} F(\theta) = \sum_{k=1}^K \frac{|D_k|}{|\mathcal{D}|} F_k(\theta) \quad , \quad (1)$$

$$F_k(\theta) = \frac{1}{|D_k|} \sum_{(x, y_i) \in D_k} \ell(f_k(\theta, x_i), y_i)$$

where  $|\mathcal{D}| = \sum_{k=1}^K |\mathcal{D}_k|$  and  $F(\theta)$  is the global loss function of *FedAvg* [32]. FL is performed in an iterative fashion. At each round, each client downloads the current version of the global model and trains it using their local data. Clients then send the updated model parameters to the central server. The central server uses the model updates from the selected clients and aggregates them to update the global model. Iterations continue until convergence.

In Equation 1, the assumption is that the data is collected from an IID distribution, and all clients should train their data according to the exact same model. However, this assumption cannot be applied within many practical FL settings due to the non-IID nature of data and resource limitations [17, 18]. In the PFL settings with high heterogeneity and non-IID data distribution, the same issue persists and the local parameters need to be customized toward each agent. PFL extends FL by solving the following [26, 34]:

$$\min_{\theta, \theta_k} \sum_{k=1}^K \frac{1}{|\mathcal{D}_k|} (\mathcal{F}_k(\theta_k) + \alpha_k \|\theta_k - \theta\|^2). \quad (2)$$

PFL explicitly handles data heterogeneity through the term  $\mathcal{F}_k(\theta_k)$  which accounts for model heterogeneity by considering personalized parameter  $\theta_k$  for client  $k$ . Meanwhile,  $\theta$  represents the shared global model parameters in Equation 2, and  $\alpha_k$  acts as a regularizer and indicates the degree of personalization tuning collaborative learning between personalized local models  $\theta_k$  and generalized global model  $\theta$ . When  $\alpha_k$  is small, the personalization power of the local models will be increased. If  $\alpha_k$  is large, the local models' parameters tend to be closer to the global model parameters  $\theta$ .

### 3.1. Partial Personalized Model

The limitations of full model personalization methods with global and fully independent local models are discussed in Section 7. Partial PFL methods improve personalization by providing more flexibility through allowing clients to choose which parts of their models to be personalized based on their specific needs and constraints for improved performance. Let  $L_k^t$  be a partial local model  $k$  in round  $t$  which is partitioned into two parts  $\langle L_{l,k}^t; L_{g,k}^t \rangle$ , where  $l, g \subseteq \{1, \dots, M\}$  are the personalized and global layers, and  $M$  is the number of layers. We can integrate both personalized and generalized layers in a local model  $L_k$  as:

$$\mathcal{F}_k(\theta_k) = \ell(f_k(\langle L_{g,k}; L_{l,k} \rangle, x_k), y_k) \quad (3)$$

Among different partitioning strategies for partial PFL [34], the most popular technique is to assign local personalized layers  $L_{l,k}^t$  to final layers and allow the base layers  $L_{g,k}^t$  to share the knowledge similar to *FedPer* [4]. This

choice aligns with insights from MAML<sup>3</sup> algorithm, suggesting that initial layers keep general and broad information while personalized characteristics manifest prominently in the higher layers. Accordingly, we would have:

$$\mathcal{F}_k(\theta_k) = L_l^{(t)}(L_g^{(t)}(x_k)) \xrightarrow{\text{localupdate}} L_l'(L_g'(x_k)) \quad ,$$

$$L_l'(L_g'(x_k)) \xrightarrow{\text{broadcasting}} L_l^{(t+1)}(G^{(t+1)}(x_k))$$

For simplicity  $L_g = L_{g,k}$  and  $L_l = L_{l,k}$  where  $\{1 \leq g \leq s \leq l \leq M\}$  and  $s$  is the split(cut) layer. The objective in solving Equation 3.1 is to find the optimal  $s$  (cut layer) which minimizes the personalization objective:  $\sum_{k=1}^K \frac{1}{|\mathcal{D}_k|} \mathcal{F}_k(\theta_k) = L_l^{(t)}(L_g^{(t)}(x_k))$ .

In partial models, after several rounds of local training, both personalized and global layers of local model are updated. This update could be synchronous like *FedSim* or asynchronous as in *FedAlt*. The Personalized layers will be frozen until the next communication round,  $L_l^{(t+1)} = L_l'$  and the global layers will be sent to the server for global model aggregation:  $G^{(t+1)} \leftarrow \sum_{k=1}^K \frac{|\mathcal{D}_k|}{|\mathcal{D}|} L_g'(x_k)$ . In the next broadcasting phase, the shared layers of the local model will be updated as  $L_g^{(t+1)} \leftarrow G^{(t+1)}$ . Our goal is to benefit from Mixup to improve personalization.

## 4. The Proposed Method

### 4.1. Mixup

Mixup is a data augmentation technique for enhancing model generalization [61] based on learning to generalize on linear combinations of training examples. Variations of Mixup have consistently excelled in vision tasks, contributing to improved robustness, generalization, and adversarial privacy. Mixup creates augmented samples as:

$$\begin{aligned} \bar{x} &= \lambda.x_i + (1 - \lambda).x_j \\ \bar{y} &= \lambda.y_i + (1 - \lambda).y_j, \end{aligned} \quad (4)$$

where  $x_i$  and  $x_j$  are two input samples,  $y_i$  and  $y_j$  are the corresponding labels,  $\lambda, \lambda \sim \text{Beta}(\alpha, \alpha), \lambda \in [0, 1]$ , is the degree of interpolation between the two samples. Mixup relates data points belonging to different classes which has been shown to be successful in mitigating overfitting and improving model generalization [13, 49, 62]. There are many variants of Mixup that has been developed to address specific challenges and enhance its effectiveness. For instance, AlignMixup [48] improves local spatial alignment by introducing transformations that better preserve semantic consistency between input pairs. Manifold Mixup [49] extends the concept to hidden layer representations, acting as a powerful regularization technique by training deep neural networks (DNNs) on linear combinations of intermediate features. CutMix [60] replaces patches between

<sup>3</sup>Model-Agnostic Meta-Learning



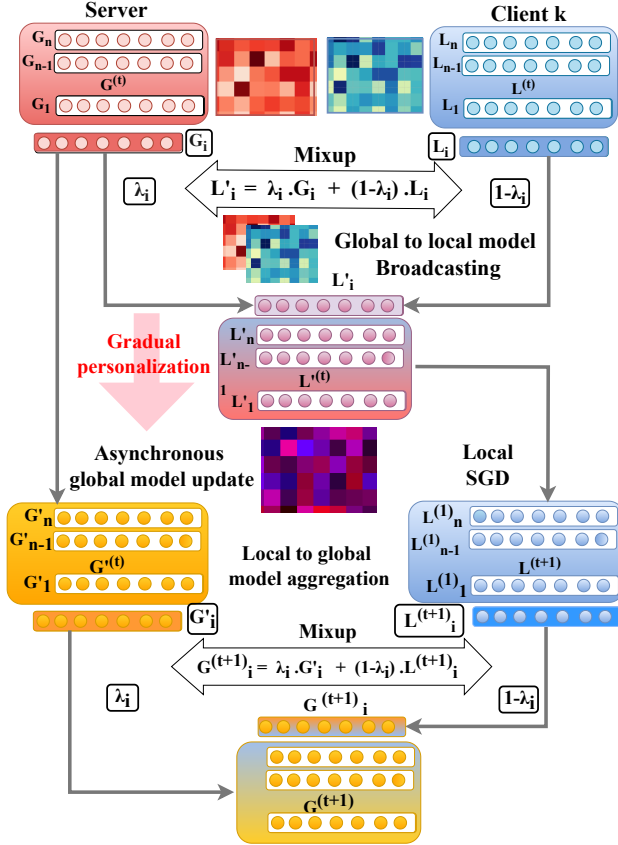


Figure 2. Workflow of pMixFed: Mixup is used in two stages. **1-Broadcasting:** when transferring knowledge to local models, the frozen personalized model  $L_k^{(t)}$  is mixed up with global model  $G^{(t)}$  according to the adaptive mix factor  $\mu_k^{(t)}$  which determines layer-wise mixup degree  $\lambda_i$  for layer  $i$ . **2-Aggregation:** The updated global model  $G^{(t+1)}$  is generated through a Mixup between the updated local model  $L^{(t+1)}$  and the current shared global model  $G^{(t)}$ . Consequently, a state of the previous global model  $G^{(t)}$  is retained, which aids in mitigating catastrophic forgetting.

images, blending visual information while retaining spatial structure. Remix [7] addresses class imbalance by assigning higher weights to minority classes during the mixing process, enhancing the robustness of the trained model on imbalanced datasets. AdaMix [13] dynamically optimizes the mixing distributions, reducing overlaps and improving training efficiency. This linear interpolation also serves as a regularization technique that shapes smoother decision boundaries, thereby enhancing the ability of a trained model to generalize to unseen data. Mixup can also increase robustness against adversarial attacks [5, 62]; and improves performance against noise, corrupted labels, and uncertainty as it relaxes the dependency on specific information [13].

## 4.2. pMixFed : Partial Mixed up Personalized federated learning

Our goal is to leverage the well-established benefits of Mixup in the context of personalized FL. While Mixup has previously been employed in FL frameworks, such as XORMixup [40], FEDMIX [57], and FedMix [51], prior studies have primarily focused on using Mixup for data augmentation or data averaging. We propose **pMixFed** by integrating Mixup on the model parameter space, rather using it on the feature space. We apply Mixup between the parameters of the global and the local models in a layer-wise manner for more customized and adaptive PFL. Our approach eliminates the need for static and rigid partitioning strategies. Specifically, during both the broadcasting and aggregation stages of our partial PFL framework, we generate mixed model weights using an interpolation strategy which is illustrated in Figure 2. Mixup offers the flexibility in combining models by introducing a mix degree for each layer  $\lambda_i$ , which changes gradually according to  $\mu$ , i.e., the *mix factor*. Parameter  $\mu$  is also updated adaptively in each communication round and for each client according to the test accuracy of the global and the local model during the evaluation phase of FL.  $\mu$  is computed as follows:

$$\mu_k^t = 1 - \frac{1}{1 + e^{-\delta(Acc_k^t - 1)}} \quad (5)$$

$\delta = (t/T)$ , where  $t$ , and  $T$  are the current communication round, and the overall number of communication rounds respectively. Also,  $Acc$  calculated as:  $Acc = (Acc_k^t / Acc_{overall}^{(t-1)})$  in the *broadcasting* phase and average test accuracy of the previous global model ( $Acc = G^t(x, \theta^t), y$ ) on all local test sets  $x = \{x_1, x_2, \dots, x_K\}$ , in the *aggregation* stage.  $b$  is the offset parameter for sigmoid function which is set to 2 after several experiments. More detailed discussion on parameter  $\mu$ 's rule of update is discussed in section 5.4 and the reason behind this formulation is discussed in the Appendix 8.

As shown in Figure 2, Mixup is applied in two distinct stages of FL. Firstly, when transferring shared knowledge to local models, the local model  $L_k$  is mixed up with the current global model  $G$  according to the dynamic mixing factor  $\mu$ , which determines the change ratio of  $\lambda_i$  (layer-wise Mixup degree in Eq. (4)) across different layers.  $\lambda_i$  gradually is changed from  $1 \rightarrow 0$  as we move from the head to the base layer.  $\lambda_i = 1$  means sharing the 100% of the global model and  $\lambda_i = 0$  means that the corresponding layer in local model is frozen and will not be mixed up with the global model  $G$ . Calculation of the Mixup degree of layer  $i$   $\lambda_i$  at both broadcasting and aggregation stages is

performed as follows:

$$\begin{aligned} \text{Broadcasting Stage: } \lambda_i &= \begin{cases} 1 & \lambda_i > 1 \\ \mu * (n - i) & \lambda_i \leq 1 \end{cases} \\ \text{Aggregation Stage: } \lambda_i &= \begin{cases} 0 & \lambda_i \leq 0 \\ 1 - (i * \mu) & \lambda_i > 0, \end{cases} \end{aligned} \quad (6)$$

where  $n$  is total number of layers,  $i$  is the current layer number starting from the base layer to the head as  $i = 0 \rightarrow i = n$ .  $\mu$  is the mix factor which will be adaptively updated in each communication round  $t$  and for each local model  $k$  according to Eq. 5.

---

#### Algorithm 1 pMixFed: Broadcasting global to local model

---

```

1: Input: Initial states global model:  $GM^{(0)}$ , local models:
    $\{LM_i^{(0)}\}_{i=1,\dots,M}$ , Number of communication rounds  $T$ , number
   of devices per round  $m$ , Number of layers in local models  $\{L_i\}$ 
2: for  $t = 0, 1, \dots, T - 1$  do
3:   Server selects  $K$  devices  $S(t) \subset \{1, \dots, N\}$ 
4:   Update  $\mu$  for each  $LM_i$ ,  $i = \{1, \dots, K\}$ 
5:   Server broadcasts  $GM^{(t)}$  to each device in  $S(t)$ 
6:   for each device  $m \in S(t)$  in parallel do
7:      $(LM_m^{(t+1)}, GM_m^{(t+1)}) = \text{Mixup}[(LM_m^{(t)}, GM_m^{(t)}), \mu]$ 
8:     Device sends  $GM_m^{(t+1)}$  back to server
9:     Update  $\mu_{i=1,\dots,K}$ 
10:  end for
11:  Server updates  $GM^{(t+1)} = \frac{1}{K} \sum_{i \in S(t)} GM_m^{(t+1)}$ 
12: end for

```

---



---

#### Algorithm 2 Proposed Mixup for Aggregation

---

```

1: Input: Initial states global model:  $GM^{(0)}$ , Number of commu-
   nication rounds  $T$ , Number of local iterations  $Itr$ , number of de-
   vices per round  $m$ , Mixup degree  $\lambda$ 
2: for  $t = 0, 1, \dots, T - 1$  do
3:   Server broadcasts  $GM^{(t)}$  to each device in  $S(t)$ :  $LM_i^{(t)}$ 
4:   Update  $\lambda_{i=1,\dots,M}$  for each device
5:   for each device  $i \in S(t)$  do
6:     for  $epoch = 0, 1, \dots, Itr - 1$  do
7:       Train local model:
8:          $LM_i^{(t+1)} = GM^{(t)}$ 
9:          $GM^{(t+1)} =$ 
10:         $\text{Mixup}(LM_i^{(t+1)}, GM^{(t)})$ 
11:     end for
12:     Device sends  $GM^{(t+1)}$  back to server
13:     Adaptively update  $\lambda_{i=1,\dots,M}$ 
14:   end for
15: end for

```

---

#### 4.2.1. Broadcasting : Global to local model transfer

This stage involves sharing global knowledge with local clients. In the existing PFL methods, the same weight allocation is typically applied to each heterogeneous local model. In our work, we personalize this process by allowing the local model to select the proportion of layers it requires. For instance, for a cold-start user, more information should be extracted from the shared knowledge model, im-

plying that a few layers should be frozen for personalization. Accordingly, A history of the previous global model  $G^t$  will remain which helps with catastrophic forgetting of the generalized model. Additionally, we introduce a gradual update procedure where the value of  $\lambda$  gradually decreases from one (indicating fully shared layers) from the base layer to the end, based on the mixing factor  $\mu$ . The mix layer is adaptively updated in each communication round for each client individually, according to personalization accuracy. With this adaptive and flexible approach, not only can upcoming streaming unseen data be managed, but also the participation gap (test accuracy of new cold start users) would be improved. The Broadcasting phase is illustrated in 1 which is inspired by [20]. The update rule of local model  $L_k^{(t)}$  is as follows:

$$\begin{aligned} L'_{k,i}{}^{(t)} &= (\lambda_{k,i}^{(t)}) \cdot G_i^{(t)} + (1 - \lambda_{k,i}^{(t)}) \cdot L_{k,i}^{(t)} \\ L_k^{(t+1)} &= L_k^{(t)} - \eta \nabla F_k(L_k^{(t)}). \end{aligned} \quad (7)$$

#### 4.2.2. Aggregation: Local to Global Model Transfer

Existing methods primarily categorize layers into two types: personalized layers and generalized layers. The updated global layers from different clients,  $G_k^{(t+1)}$ , are typically aggregated using Equation 3, which can lead to catastrophic forgetting. Since The base layers of the global model serve as the backbone of shared knowledge [37], This issue arises because, during each local update, the generalized layers undergo substantial modifications [33, 34]. When the global model is updated by simply aggregating local models, valuable information from previously shared knowledge may be lost, leading to forgetting—even if  $G^t$  performs better than the newly aggregated model. To address this challenge, we propose a new strategy that applies Mixup between the gradients of the previous global model and each client's local model before aggregation. For each client  $i$ , the mixup coefficient  $\lambda_i$  gradually increases from 0 to 1, moving from the head to the base layer, controlled by the mix factor  $\mu_i$ . Additionally, the base layer is adaptively updated based on the communication round and the generalization accuracy, ensuring robust integration of shared and personalized knowledge. It should be noted that parameter  $\mu$  is constant in the aggregation stage for all clients as it's dependent to the average performance of the previous global model.

$$\begin{aligned} G'_{k,i}{}^{(t)} &= (\lambda_{i,k}^{(t)}) \cdot G_i^{(t)} + (1 - \lambda_{i,k}^{(t)}) \cdot L_{k,i}^{(t+1)}, \\ G^{(t+1)} &= \sum_{k=1}^K \frac{|D_k|}{\sum_{k=1}^K |D_k|} G_k^{(t+1)}. \end{aligned} \quad (8)$$

The high-level block-diagram visualization of the proposed method is shown in Figure 2. It is important to note that the sizes of local models  $LM_i^{(0)}$  can differ from each other. Consequently, the size of  $GM^{(0)}$  should be greater than the maximum size of local models. The parameter

$\lambda$  in Equation 4 determines the Mixup degree between the shared model  $GM$  and the local models  $LM_i^{(c)}$ , while  $\mu$  governs the slope of the change in  $\lambda$  across different layers. The degree of Mixup gradually decreases according to the parameter  $\mu$  from 0 to 1. In this scenario,  $\lambda = 0$  for the first base layer, indicating total sharing, while  $\lambda = 1$  applies to the final layer, which represents no sharing. The underlying concept is that the base layer contains more general information, whereas the final layers retain client-specific information. The use of the parameter  $\mu$ , relative to the number of local layers, eliminates the need for a specified cut layer  $k$  and allows its application across different model sizes and layers. The parameter  $\mu_i$  is adaptively updated based on the personalized and global model accuracy for each client. Algorithm 1 shows how Mixup is used as a shared aggregation technique between individual clients and the server. In each training round, only one client is *Mixed up* with the global model, and  $\lambda$  is adaptively learned based on the objective function using online learning. Algorithm 2 shows how Mixup is employed as a shared aggregation technique between the clients and the server. In each training round, only one client is “Mixed up” with the global model and the  $\lambda$  parameter is adaptively learned based on the objective function using online learning. For a **theoretical convergence analysis** of *pMixFed*, please refer to the Appendix 9.

## 5. Experiments

### 5.1. Experimental Setup

**Datasets:** We used three datasets widely used federated learning: **MNIST** [23], **CIFAR-10**, and **CIFAR-100** [3]. We followed the setup in [32] and [33] to simulate heterogeneous, non-IID data distributions across clients for both train and test datasets. The maximum number of classes per user is set to  $S = 5$  for CIFAR-10 and MNIST, and  $S = 50$  for CIFAR-100. Experiments were conducted across varying heterogeneous settings, including small-scale ( $N = 10$ ) and large-scale ( $N = 100$ ) client populations, with different client participation rates  $C = [100\%, 10\%]$  to measure the effects of stragglers.

**Baselines and backbone:** We compare two version of our method (i) **pMixFed**: an adaptive and dynamic mixup-based PFL approach, and (ii) **pMixFed-Dynamic**: a dynamic-only mixup variant where the parameter  $\mu$  is fixed across communication rounds, against several baselines. These baselines include: **FedAvg** [32], **FedAlt** [34], **FedSim** [34], **FedBABU** [33]. Additionally, we compare against full model personalization methods, **Ditto** [28], **Per-FedAvg** [12], and **LG-FedAvg** [29]. For all experiments, the number of local training epochs was set to  $r = 5$ , number of communication rounds was fixed at  $T = 100$ , and the batch size was 32. The Adam optimizer has been used

while the learning rate, for both global and local updates, was  $lr = 0.001$  across all communication rounds. The average personalized test accuracy across individual client’s data in the final communication round is reported in Table 2 and 1. Figure 3 presents the training accuracy versus communication rounds for CIFAR10 and CIFAR100 datasets.

**Model Architectures:** Following the FL literature, we utilized several model architectures. For MNIST, we used a simple CNN consisting of 2 convolutional layers (each with 1 block) and 2 fully connected layers. for CIFAR10 and CIFAR100, We employed a CNN with 4 convolutional layers (1 block each) and 1 fully connected layer for all datasets. Additionally, we used MobileNet, which comprises 14 convolutional layers (2 blocks each) and 1 fully connected layer, for CIFAR-10 and CIFAR-100. For partial model approaches such as **FedAlt** and **FedSim**, the split layer is fixed in the middle of the network: for CNNs, layers [1,2] are shared, while for MobileNet, layers [1–7] are considered as shared part. More details about the training process is discussed in Appendix 10.1. Our implementation is available as a supplement for reprodcng the results.

### 5.2. Comparative Results

We evaluate two versions of our proposed method: **pMixFed**, which utilizes both adaptive and dynamic layer-wise mixup degree updates, and **pMixFed-Dynamic**, where the mixup coefficient  $\mu_i$  is fixed across all training rounds and gradually decreases from  $1 \rightarrow 0$  from the head to the base layer ( $i = M \rightarrow 1$ ) following a Sigmoid function designed for each client. Our results show that the final accuracy of *pMixFed* outperforms baseline methods in most cases. As shown in Figure 3, the accuracy curve of *pMixFed* exhibits smoother and faster convergence, which may suggest the potential for early stopping in FL settings. Previous studies on mixup also suggest that linear interpolation between features provides the most benefit in the early training phase [65]. Moreover, Figure 3 highlights that partial models with a hard split are highly sensitive to hyperparameter selection and different distribution settings, which can lead to training instability. This issue appears to be addressed more effectively in *pMixFed*, as discussed further in Section 5.3. According to the results in Table 2 and Table 1, *Ditto* demonstrates relatively robust performance across different heterogeneity settings. However, its effectiveness diminishes as the model depth increases, such as with MobileNet, and under larger client populations ( $N = 100$ ). On the other hand, while *FedAlt* and *FedSim* report above-baseline results, they consistently fail during training. Adjusting hyperparameters did not resolve this issue.

### 5.3. Analytic Experiments

**Adaptive Robustness to Performance Degradation:** During our experiments, we observed the algorithm’s abil-

Table 1. Comparison of the State-of-The-Art Methods using Mobile-Net model

Method	CIFAR-10				CIFAR-100			
	$N = 100$		$N = 10$		$N = 100$		$N = 10$	
	$C = 10\%$	$C = 100\%$	$C = 10\%$	$C = 100\%$	$C = 10\%$	$C = 100\%$	$C = 10\%$	$C = 100\%$
FedAvg	26.93	25.61	15.64	19.55	4.50	4.54	17.65	21.24
FedAlt	39.36	46.06	39.60	42.79	27.85	19.07	48.30	14.31
FedSim	51.12	45.43	40.30	35.43	28.18	19.52	47.41	48.30
FedBaBU	28.70	25.98	17.58	20.74	4.63	4.72	17.46	17.57
Ditto	26.58	62.77	18.60	43.98	7.00	16.07	16.89	20.74
Per-FedAvg	34.30	43.59	19.52	38.29	24.04	30.65	16.27	37.20
Lg-FedAvg	34.52	34.17	48.88	58.51	5.65	5.73	31.89	35.78
<b>pMixFed</b>	<b>69.94</b>	<b>72.42</b>	<b>54.90</b>	<b>74.62</b>	<b>45.62</b>	<b>56.63</b>	<b>54.71</b>	<b>58.25</b>

Table 2. Comparison of the State-of-The-Art Methods using CNN model

Method	CIFAR-10				CIFAR-100				MNIST	
	$N = 100$		$N = 10$		$N = 100$		$N = 10$		$N = 100$	$N = 10$
	$C = 10\%$	$C = 100\%$	$C = 10\%$	$C = 100\%$	$C = 10\%$	$C = 100\%$	$C = 10\%$	$C = 100\%$	$C = 100\%$	$C = 100\%$
FedAvg	54.78	56.82	44.11	54.37	25.77	26.73	34.47	39.93	97.54	98.59
FedAlt	56.41	56.77	69.50	64.80	15.19	10.56	28.30	26.53	97.37	99.21
FedSim	59.90	56.07	63.46	38.34	14.80	10.46	27.00	26.47	98.63	99.60
FedBaBU	53.12	54.60	39.77	53.21	16.77	17.33	25.60	32.47	98.19	99.07
Ditto	46.86	<b>79.60</b>	31.65	60.75	27.16	<b>42.93</b>	25.38	55.27	98.03	95.51
Per-FedAvg	39.37	45.03	10.00	48.13	32.67	39.01	8.71	41.21	98.32	50.34
Lg-FedAvg	62.28	62.99	62.46	71.73	28.75	28.03	33.75	45.76	97.65	98.82
<b>pMixFed</b>	<b>65.30</b>	<b>75.49</b>	<b>74.36</b>	<b>75.06</b>	<b>34.66</b>	41.56	<b>43.47</b>	<b>51.46</b>	<b>99.88</b>	<b>99.98</b>

ity to adapt and recover from performance degradation, especially in challenging scenarios such as gradient vanishing, adding new users, or introducing unseen incoming data. For instance, in complex settings with larger models, such as *MobileNet* on the CIFAR-100 dataset, partial PFL models like *FedSim* and *FedAlt* experience sudden accuracy drops due to zero gradients or the incorporation of new participants into the cohort. We believe the reason behind this phenomenon is due to the: 1-local and global model update discrepancy in partial models with strict cut in the middle depicted in Figure 1. This degradation is mitigated by the adaptive mixup coefficient, which dynamically adjusts the degree of personalization based on the local model’s performance during both the broadcasting and aggregation stages. Specifically, if the global model  $G^{(t)}$  lacks sufficient strength, the mixup coefficient  $\mu^{(t)}$  is reduced, decreasing the influence of global model. 2- Catastrophic forgetting which is addressed in *pMixFed* by keeping the historical models  $H_1^T G^t$  in the aggregation process as discussed in section 4.2.2. Figure 4 illustrates that even applying mixup only to the shared layers of the same partial PFL models (*FedAlt* and *FedSim*) enhances resilience against sudden accuracy drops, maintaining model performance over time. In both experiments, the mixup degree for personalized layers is set to  $\lambda_i = 0$  for all clients similar to *FedSim* and *FedAlt* algorithms.

## 5.4. Ablation Study

**Random vs gradual mix factor from  $\beta$  distribution:** In this paper, we have explored different designs for calculating g mix factor  $\mu_k$ . The value of  $\lambda$  in Eq. 4, naturally sampled from a  $\beta \neq (\alpha, \alpha)$  distribution [61] which is on the interval  $[0,1]$ . We have also experimented the random  $\lambda_i$  using  $\beta$  distribution with different  $\alpha$ . If  $\alpha = 1$ , the  $\beta$  distribution is uniform meaning that the  $\lambda$  would be sampled uniformly from  $[0,1]$ . Moreover  $\alpha > 1$ , The  $\lambda$  would be more in between, creating a more mixed output between  $L_k$  and  $G$ . On the contrary, if  $\alpha < 1$  the mixed model tend to choose just one of the global and local models where  $\lambda = 1$  or  $\lambda = 0$ . The effects of different  $\alpha$  on mixup degree  $\lambda$  is discussed in Appendix.

**Mix Factor( $\mu$ ): sigmoid vs Dynamic-only** In this study, we have exploited two different functions to update adaptive mixup factor( $\mu$ ) in each communication round. This idea is based on the performance of the model which we want to update. In 1st scenario  $\sigma$  function has been adapted as shown in equation 5 for adaptively updating mixup degree  $\lambda_i$  using sigmoid function. On the other hand, the 2nd scenario, Dynamic-only,  $Mu$  is fixed over all communication rounds. The comparison of these two scenarios as well as the effect of different  $t$  values on the test accuracy, is depicted in Figure 5 (b).



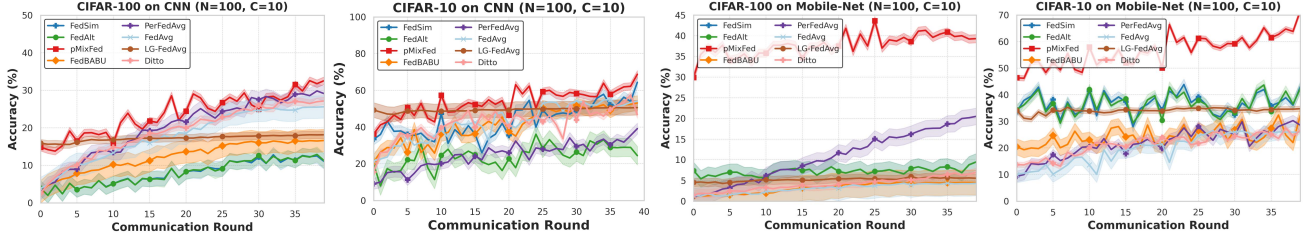


Figure 3. test accuracy accuracy curve along with global communication rounds for  $pMixFed$  and PFL baselines experimented on CIFAR10 and CIFAR100 where  $N=100, C=10\%$ .

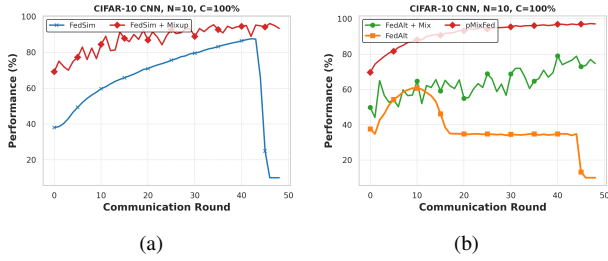


Figure 4. (a) The accuracy drop in FedSim occurred due to the vanishing gradient at round 42. (b) accuracy declines at round 10 in FedAlt due to the introduction of 5 new participants. Applying adaptive mixup solely between corresponding global and local shared layers mitigates the accuracy drop.

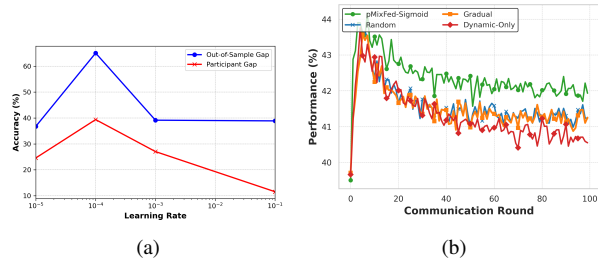


Figure 5. (a) Effect on learning rate on average test accuracy(out-of-sample) gap and on the cold-start users. (b) The comparison between test accuracy on the cold-start-users with different  $Mix$  factor functions. (Dynamic-only). In this scenario we used a fixed  $Mu$  for all communication rounds. (Sigmoid). The original updating strategy based on a sigmoid function. (Gradual). A simple linear function has been adapted for updating  $Mu$ . (Random) Mixup degree  $\lambda_i$  is selected randomly from  $\beta$  distribution.

**Effect of Mixup Degree as Learning Rate ( $\Gamma$ ):** We observed that the effect of the mixup coefficient is highly influenced by the learning rate and its decay. To empirically demonstrate this relationship, we measured the impact of the learning rate on new participants (cold-start users) as well as on the out-of-sample gap (average test accuracy on unseen data). The results of this comparison are presented in Figure 5 (a). Additional details are provided in the Appendix 10.3.

## 6. Conclusions

We introduced  $pMixFed$ , a dynamic, layer-wise personalized federated learning approach that uses mixup to integrate the shared global and personalized local models. Our approach features adaptive partitioning between shared and personalized layers, along with a gradual transition for personalization, enabling seamless adaptation for local clients, improved generalization across clients, and reduced risk of catastrophic forgetting. We provided a theoretical analysis of  $pMixFed$  to study the properties of its convergence. Our experiments on three datasets demonstrated its superior performance over existing PFL methods. Empirically,  $pMixFed$  exhibited faster training times, increased robustness, and better handling of data heterogeneity compared to state-of-the-art PFL models. Future research directions include exploring multi-Modal personalization and adapting  $pMixFed$  for working on resource-constrained devices

## 7. Acknowledgment

This work is based upon the work partly supported by the National Center for Transportation Cybersecurity and Resiliency (TraCR) (a U.S. Department of Transportation National University Transportation Center) headquartered at Clemson University, Clemson, South Carolina, USA. Any opinions, findings, conclusions, and recommendations expressed in this material are those of the author(s) and do not necessarily reflect the views of TraCR, and the U.S. Government assumes no liability for the contents or use thereof.

## References

- [1] Sawsan Abdulrahman, Hanine Tout, Azzam Mourad, and Chamseddine Talhi. Fedmccs: Multicriteria client selection model for optimal iot federated learning. *IEEE Internet of Things Journal*, 8(6):4723–4735, 2021. 3
- [2] Alekh Agarwal, John Langford, and Chen-Yu Wei. Federated residual learning. *arXiv preprint arXiv:2003.12880*, 2020. 3
- [3] Krizhevsky Alex. Learning multiple layers of features from tiny images. <https://www.cs.toronto.edu/kriz/learning-features-2009-TR.pdf>, 2009. 7, 6

- [4] Manoj Ghuhan Arivazhagan, Vinay Aggarwal, Aaditya Kumar Singh, and Sunav Choudhary. Federated learning with personalization layers. *arXiv preprint arXiv:1912.00818*, 2019. 2, 3, 4, 1
- [5] Christopher Beckham, Sina Honari, Vikas Verma, Alex M Lamb, Farnoosh Ghadiri, R Devon Hjelm, Yoshua Bengio, and Chris Pal. On adversarial mixup resynthesis. *Advances in neural information processing systems*, 32, 2019. 5
- [6] Duc Bui, Kshitiz Malik, Jack Goetz, Honglei Liu, Seungwhan Moon, Anuj Kumar, and Kang G Shin. Federated user representation learning. *arXiv preprint arXiv:1909.12535*, 2019. 3
- [7] Hsin-Ping Chou, Shih-Chieh Chang, Jia-Yu Pan, Wei Wei, and Da-Cheng Juan. Remix: rebalanced mixup. In *Computer Vision—ECCV 2020 Workshops: Glasgow, UK, August 23–28, 2020, Proceedings, Part VI 16*, pages 95–110. Springer, 2020. 5
- [8] Gregory Cohen, Saeed Afshar, Jonathan Tapon, and Andre Van Schaik. Emnist: Extending mnist to handwritten letters. In *2017 international joint conference on neural networks (IJCNN)*, pages 2921–2926. IEEE, 2017. 6
- [9] Liam Collins, Hamed Hassani, Aryan Mokhtari, and Sanjay Shakkottai. Exploiting shared representations for personalized federated learning. In *International conference on machine learning*, pages 2089–2099. PMLR, 2021. 2
- [10] Liam Collins, Aryan Mokhtari, Sewoong Oh, and Sanjay Shakkottai. Maml and anil provably learn representations. In *International Conference on Machine Learning*, pages 4238–4310. PMLR, 2022. 1, 6
- [11] Moming Duan, Duo Liu, Xianzhang Chen, Yujuan Tan, Jinting Ren, Lei Qiao, and Liang Liang. Astraea: Self-balancing federated learning for improving classification accuracy of mobile deep learning applications. In *2019 IEEE 37th international conference on computer design (ICCD)*, pages 246–254. IEEE, 2019. 3
- [12] Alireza Fallah, Aryan Mokhtari, and Asuman Ozdaglar. Personalized federated learning: A meta-learning approach. *arXiv preprint arXiv:2002.07948*, 2020. 3, 7
- [13] Hongyu Guo, Yongyi Mao, and Richong Zhang. Mixup as locally linear out-of-manifold regularization. In *Proceedings of the AAAI conference on artificial intelligence*, pages 3714–3722, 2019. 4, 5
- [14] Chaoyang He, Murali Annavaram, and Salman Avestimehr. Group knowledge transfer: Federated learning of large cnns at the edge. *Advances in Neural Information Processing Systems*, 33:14068–14080, 2020. 3
- [15] Wenke Huang, Mang Ye, and Bo Du. Learn from others and be yourself in heterogeneous federated learning. In *Proceedings of the IEEE/CVF Conference on Computer Vision and Pattern Recognition*, pages 10143–10153, 2022. 1, 2
- [16] Yutao Huang, Lingyang Chu, Zirui Zhou, Lanjun Wang, Jiangchuan Liu, Jian Pei, and Yong Zhang. Personalized cross-silo federated learning on non-iid data. In *Proceedings of the AAAI conference on artificial intelligence*, pages 7865–7873, 2021. 3
- [17] Ahmed Imteaj and M Hadi Amini. Fedparl: Client activity and resource-oriented lightweight federated learning model for resource-constrained heterogeneous iot environment. *Frontiers in Communications and Networks*, 2: 657653, 2021. 4
- [18] Ahmed Imteaj, Urmish Thakker, Shiqiang Wang, Jian Li, and M Hadi Amini. A survey on federated learning for resource-constrained iot devices. *IEEE Internet of Things Journal*, 9(1):1–24, 2021. 4
- [19] Eunjeong Jeong, Seungeun Oh, Hyesung Kim, Jihong Park, Mehdi Bennis, and Seong-Lyun Kim. Communication-efficient on-device machine learning: Federated distillation and augmentation under non-iid private data. *arXiv preprint arXiv:1811.11479*, 2018. 3
- [20] Peter Kairouz, H Brendan McMahan, Brendan Avent, Aurélien Bellet, Mehdi Bennis, Arjun Nitin Bhagoji, Kallista Bonawitz, Zachary Charles, Graham Cormode, Rachel Cummings, et al. Advances and open problems in federated learning. *Foundations and Trends® in Machine Learning*, 14(1–2):1–210, 2021. 6
- [21] Sai Praneeth Karimireddy, Satyen Kale, Mehryar Mohri, Sashank Reddi, Sebastian Stich, and Ananda Theertha Suresh. Scaffold: Stochastic controlled averaging for federated learning. In *International conference on machine learning*, pages 5132–5143. PMLR, 2020. 3
- [22] Jakub Konečný, H Brendan McMahan, Felix X Yu, Peter Richtárik, Ananda Theertha Suresh, and Dave Bacon. Federated learning: Strategies for improving communication efficiency. *arXiv preprint arXiv:1610.05492*, 2016. 1
- [23] Yann LeCun, Léon Bottou, Yoshua Bengio, and Patrick Haffner. Gradient-based learning applied to document recognition. *Proceedings of the IEEE*, 86(11):2278–2324, 1998. 7, 6
- [24] Sunwoo Lee, Anit Kumar Sahu, Chaoyang He, and Salman Avestimehr. Partial model averaging in federated learning: Performance guarantees and benefits. *Neurocomputing*, 556: 126647, 2023. 2
- [25] Daliang Li and Junpu Wang. Fedmd: Heterogenous federated learning via model distillation. *arXiv preprint arXiv:1910.03581*, 2019. 3
- [26] Qinbin Li, Bingsheng He, and Dawn Song. Model-contrastive federated learning. In *Proceedings of the IEEE/CVF conference on computer vision and pattern recognition*, pages 10713–10722, 2021. 3, 4
- [27] Tian Li, Anit Kumar Sahu, Manzil Zaheer, Maziar Sanjabi, Ameet Talwalkar, and Virginia Smith. Federated optimization in heterogeneous networks. *Proceedings of Machine learning and systems*, 2:429–450, 2020. 3
- [28] Tian Li, Shengyuan Hu, Ahmad Beirami, and Virginia Smith. Ditto: Fair and robust federated learning through personalization. In *International Conference on Machine Learning*, pages 6357–6368. PMLR, 2021. 3, 7
- [29] Paul Pu Liang, Terrance Liu, Liu Ziyin, Nicholas B Allen, Randy P Auerbach, David Brent, Ruslan Salakhutdinov, and Louis-Philippe Morency. Think locally, act globally: Federated learning with local and global representations. *arXiv preprint arXiv:2001.01523*, 2020. 2, 3, 7
- [30] Tao Lin, Lingjing Kong, Sebastian U Stich, and Martin Jaggi. Ensemble distillation for robust model fusion in fed-

- erated learning. *Advances in neural information processing systems*, 33:2351–2363, 2020. 3
- [31] Kangyang Luo, Xiang Li, Yunshi Lan, and Ming Gao. Gradma: A gradient-memory-based accelerated federated learning with alleviated catastrophic forgetting. In *Proceedings of the IEEE/CVF Conference on Computer Vision and Pattern Recognition*, pages 3708–3717, 2023. 1, 2
- [32] Brendan McMahan, Eider Moore, Daniel Ramage, Seth Hampson, and Blaise Aguera y Arcas. Communication-efficient learning of deep networks from decentralized data. In *Artificial intelligence and statistics*, pages 1273–1282. PMLR, 2017. 1, 4, 7
- [33] Jaehoon Oh, Sangmook Kim, and Se-Young Yun. Fedbabu: Towards enhanced representation for federated image classification. *arXiv preprint arXiv:2106.06042*, 2021. 3, 6, 7, 1
- [34] Krishna Pillutla, Kshitiz Malik, Abdel-Rahman Mohamed, Mike Rabbat, Maziar Sanjabi, and Lin Xiao. Federated learning with partial model personalization. In *International Conference on Machine Learning*, pages 17716–17758. PMLR, 2022. 2, 3, 4, 6, 7, 1
- [35] Sone Kyaw Pye and Han Yu. Personalised federated learning: A combinational approach. *arXiv preprint arXiv:2108.09618*, 2021. 2
- [36] Liangqiong Qu, Yuyin Zhou, Paul Pu Liang, Yingda Xia, Feifei Wang, Ehsan Adeli, Li Fei-Fei, and Daniel Rubin. Rethinking architecture design for tackling data heterogeneity in federated learning. In *Proceedings of the IEEE/CVF conference on computer vision and pattern recognition*, pages 10061–10071, 2022. 1
- [37] Aniruddh Raghu, Maithra Raghu, Samy Bengio, and Oriol Vinyals. Rapid learning or feature reuse? towards understanding the effectiveness of maml. *arXiv preprint arXiv:1909.09157*, 2019. 6
- [38] Mohammad Rostami, Soheil Kolouri, Kyungnam Kim, and Eric Eaton. Multi-agent distributed lifelong learning for collective knowledge acquisition. In *Proceedings of the 17th International Conference on Autonomous Agents and Multi-Agent Systems*, pages 712–720, 2018. 1
- [39] Aviv Shamsian, Aviv Navon, Ethan Fetaya, and Gal Chechik. Personalized federated learning using hypernetworks. In *International Conference on Machine Learning*, pages 9489–9502. PMLR, 2021. 3
- [40] MyungJae Shin, Chihoon Hwang, Joongheon Kim, Jihong Park, Mehdi Bennis, and Seong-Lyun Kim. Xor mixup: Privacy-preserving data augmentation for one-shot federated learning. *arXiv preprint arXiv:2006.05148*, 2020. 5
- [41] Nasim Shirvani-Mahdavi, Farahnaz Akrami, Mohammed Samiul Saeef, Xiao Shi, and Chengkai Li. Comprehensive analysis of freebase and dataset creation for robust evaluation of knowledge graph link prediction models. In *International Semantic Web Conference*, pages 113–133. Springer, 2023. 2
- [42] Neta Shoham, Tomer Avidor, Aviv Keren, Nadav Israel, Daniel Benditkis, Liron Mor-Yosef, and Itai Zeitak. Overcoming forgetting in federated learning on non-iid data. *arXiv preprint arXiv:1910.07796*, 2019. 3
- [43] Karan Singhal, Hakim Sidahmed, Zachary Garrett, Shanshan Wu, John Rush, and Sushant Prakash. Federated reconstruction: Partially local federated learning. *Advances in Neural Information Processing Systems*, 34:11220–11232, 2021. 1, 3
- [44] Virginia Smith, Chao-Kai Chiang, Maziar Sanjabi, and Ameet S Talwalkar. Federated multi-task learning. *Advances in neural information processing systems*, 30, 2017. 3
- [45] Guangyu Sun, Matias Mendieta, Jun Luo, Shandong Wu, and Chen Chen. Fedperfix: Towards partial model personalization of vision transformers in federated learning. In *Proceedings of the IEEE/CVF International Conference on Computer Vision*, pages 4988–4998, 2023. 2, 1
- [46] Canh T Dinh, Nguyen Tran, and Josh Nguyen. Personalized federated learning with moreau envelopes. *Advances in Neural Information Processing Systems*, 33:21394–21405, 2020. 3
- [47] Alysa Ziyang Tan, Han Yu, Lizhen Cui, and Qiang Yang. Towards personalized federated learning. *IEEE Transactions on Neural Networks and Learning Systems*, 2022. 2, 3
- [48] Shashanka Venkataramanan, Ewa Kijak, Laurent Amsaleg, and Yannis Avrithis. Alignmixup: Improving representations by interpolating aligned features. In *Proceedings of the IEEE/CVF Conference on Computer Vision and Pattern Recognition*, pages 19174–19183, 2022. 4
- [49] Vikas Verma, Alex Lamb, Christopher Beckham, Amir Najafi, Ioannis Mitliagkas, David Lopez-Paz, and Yoshua Bengio. Manifold mixup: Better representations by interpolating hidden states. In *International conference on machine learning*, pages 6438–6447. PMLR, 2019. 4
- [50] Han Wang, Luis Muñoz-González, David Eklund, and Shahid Raza. Non-iid data re-balancing at iot edge with peer-to-peer federated learning for anomaly detection. In *Proceedings of the 14th ACM Conference on Security and Privacy in Wireless and Mobile Networks*, pages 153–163, 2021. 3
- [51] Jeffrey Wicaksana, Zengqiang Yan, Dong Zhang, Xijie Huang, Huimin Wu, Xin Yang, and Kwang-Ting Cheng. Fedmix: Mixed supervised federated learning for medical image segmentation. *IEEE Transactions on Medical Imaging*, 42(7):1955–1968, 2022. 5
- [52] Qiong Wu, Xu Chen, Zhi Zhou, and Junshan Zhang. Fed-home: Cloud-edge based personalized federated learning for in-home health monitoring. *IEEE Transactions on Mobile Computing*, 21(8):2818–2832, 2020. 3
- [53] Peng Xiao, Samuel Cheng, Vladimir Stankovic, and Dejan Vukobratovic. Averaging is probably not the optimum way of aggregating parameters in federated learning. *Entropy*, 22(3):314, 2020. 2
- [54] Chencheng Xu, Zhiwei Hong, Minlie Huang, and Tao Jiang. Acceleration of federated learning with alleviated forgetting in local training. *arXiv preprint arXiv:2203.02645*, 2022. 2
- [55] Hongwei Yang, Hui He, Weizhe Zhang, and Xiaochun Cao. Fedsteg: A federated transfer learning framework for secure image steganalysis. *IEEE Transactions on Network Science and Engineering*, 8(2):1084–1094, 2020. 3

- [56] Xiyuan Yang, Wenke Huang, and Mang Ye. Fedas: Bridging inconsistency in personalized federated learning. In *Proceedings of the IEEE/CVF Conference on Computer Vision and Pattern Recognition*, pages 11986–11995, 2024. 2
- [57] Tehrim Yoon, Sumin Shin, Sung Ju Hwang, and Eunho Yang. Fedmix: Approximation of mixup under mean augmented federated learning. *arXiv preprint arXiv:2107.00233*, 2021. 2, 5
- [58] Tao Yu, Eugene Bagdasaryan, and Vitaly Shmatikov. Salvaging federated learning by local adaptation. *arXiv preprint arXiv:2002.04758*, 2020. 3
- [59] Honglin Yuan, Warren Morningstar, Lin Ning, and Karan Singhal. What do we mean by generalization in federated learning? *arXiv preprint arXiv:2110.14216*, 2021. 6
- [60] Sangdoon Yun, Dongyoon Han, Seong Joon Oh, Sanghyuk Chun, Junsuk Choe, and Youngjoon Yoo. Cutmix: Regularization strategy to train strong classifiers with localizable features. In *Proceedings of the IEEE/CVF international conference on computer vision*, pages 6023–6032, 2019. 4
- [61] Hongyi Zhang, Moustapha Cisse, Yann N Dauphin, and David Lopez-Paz. mixup: Beyond empirical risk minimization. *arXiv preprint arXiv:1710.09412*, 2017. 2, 4, 8
- [62] Linjun Zhang, Zhun Deng, Kenji Kawaguchi, Amirata Ghorbani, and James Zou. How does mixup help with robustness and generalization? *arXiv preprint arXiv:2010.04819*, 2020. 4, 5
- [63] Yue Zhao, Meng Li, Liangzhen Lai, Naveen Suda, Damon Civin, and Vikas Chandra. Federated learning with non-iid data. *arXiv preprint arXiv:1806.00582*, 2018. 3
- [64] Zhuangdi Zhu, Junyuan Hong, and Jiayu Zhou. Data-free knowledge distillation for heterogeneous federated learning. In *International conference on machine learning*, pages 12878–12889. PMLR, 2021. 3
- [65] Difan Zou, Yuan Cao, Yuanzhi Li, and Quanquan Gu. The benefits of mixup for feature learning. In *International Conference on Machine Learning*, pages 43423–43479. PMLR, 2023. 7



# Appendix

## 8. More Detailed discussion on the Mix Factor

This section elaborates on two key properties of *pMixFed*: 1) dynamic behavior, achieved through a gradual transition in the *mix degree* between layers ( $\lambda_i$ ), and 2) Adaptive behavior, introduced via the *mix factor* ( $\mu$ ). Below, we delve into the details and formulation of each step.

### 8.1. Dynamic Mixup Degree

Among the various partitioning strategies for partial PFL discussed in the main paper and in [34], one of the most widely adopted techniques is assigning higher layers of local model  $L_{l,k}^t$  to personalization while allowing the base layers  $L_{g,k}^t$  to be shared across clients as the global model [4, 33, 45]. This design aligns with insights from the Model-Agnostic Meta-Learning (MAML) algorithm [10], which demonstrates that lower layers generally retain task-agnostic, generalized features, while the higher layers capture task-specific, personalized characteristics. Accordingly, in this work, we designate the head of the model as containing personalized information, while the base layers represent generalized information shared across clients<sup>4</sup>.

**Broadcasting:** To achieve a nuanced and gradual transition in the mixing process between the global model and the local model, we define the mix degree  $\lambda_i$  as follows. The local model’s head  $L_n$  remains frozen, and the head of the global model is excluded from being shared with the local model. The mix degree for each layer  $\lambda_i$  increases incrementally based on the *mix factor*  $\mu$ , such that as we move toward the base layers, the personalization impact decreases. This dynamic behavior is represented as:

$$\lambda_i = \lambda_{i+1} + \mu,$$

where  $\lambda_i$  controls the degree of mixing at layer  $i$ . This process is visually illustrated in Figure 8.

**Aggregation:** The aggregation stage focuses on preserving the generalized information from the history of previous global models to mitigate the catastrophic forgetting problem. In contrast to the broadcasting process, the primary goal here is to retain the generalized information of the previous global model, which encapsulates the history of all prior models  $H_1^{t-1}G$ . Therefore, the base layers should predominantly be shared from the global model, particularly during the first round of training, where the updated local models are still underdeveloped. Nonetheless, as we transition to the head, it’s less prominent to transfer knowledge from the previous global models. Figure 8 illustrates how the mixup degree transitions from the head to the base layers.

### 8.2. Adaptive Mix-Factor

To enable online, adaptive updates of the mix degree  $\lambda_i$ , we implemented several algorithms, as detailed in Section 5.4 *Ablation Study*. We observed a clear relationship between the mixup degree and the similar behavior to lr, which is further discussed in Section 9.4.1. Inspired by learning rate schedulers, we introduced the mix-factor  $\mu$  to adaptively update the layer-wise mixup degree based on the current communication round  $\delta = t/T$  and the relative performance of the current local model  $L_k^t$  compared to the global model  $G^t$ . The Sigmoid function in Figure 8 illustrates how  $\mu$  evolves with respect to  $\delta$  and accuracy ( $Acc$ ). The best results were achieved when setting  $b = 1$  and using the square of  $Acc$  as an exponent. The rationale behind this approach is that a more experienced, better-performing model should share more information. Specifically, if the local model accuracy  $Acc_l$  significantly exceeds that of the global model ( $Acc_G$ ) in the current round ( $t$ ) such that  $Acc \gg 1$ , less information is shared from the global model. Conversely, when  $0 < Acc < 1$ , the global model dominates the parameter updates in both the global and local models. Figure 7 shows the distribution of the calculated  $\mu$  across different communication rounds for client 0 in the broadcasting stage. In the broadcasting stage, higher  $Acc_l$  values result in freezing more layers for personalization, leading to a decrease in  $\mu$ . Conversely, during the aggregation phase, if the global model accuracy  $Acc_G$  outperforms the updated local model accuracy  $Acc_l^{(t+1)}$ , more base layers are shared. This is especially important during the first round of training, where local models are less stable. As demonstrated in Section 5.3, *our proposed method adapts dynamically to performance drops and high-distribution complexity, adjusting the mixup degree as needed. This adaptability is effective even when applied partially to partial PFL methods such as FedAlt, and FedSim.*

---

<sup>4</sup>It should be noted that our method is fully adaptable to different partial PFL designs as well discussed in [34].

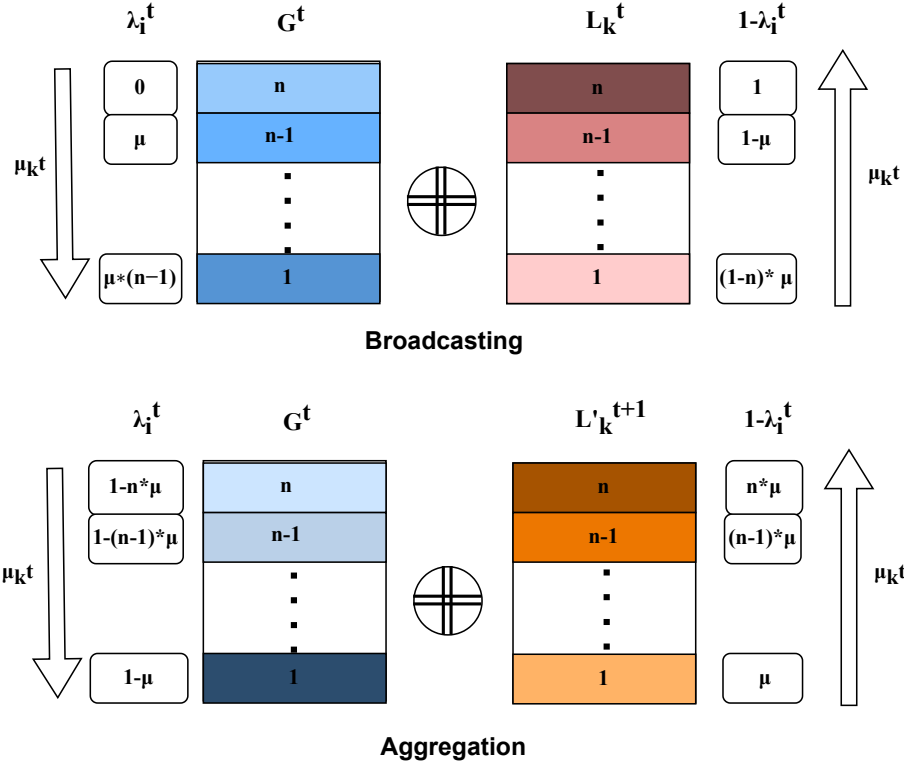


Figure 6. layer-wise Dynamic transition of mixup degree  $\lambda_i$  in Broadcasting and aggregation phase. The darker color shows the higher mixup degree ( $\lambda_i$ ) for the corresponding layer  $i$ .

### 8.3. Model Heterogeneity

$pMixFed$  is capable of handling variable model sizes across different clients. The global model,  $M_g$ , retains the maximum number of layers from all clients, i.e.,  $M_G = \max(M_1, M_2, \dots, M_N)$ . During the matching process between the global model  $G_i$  and the local model  $L_i$ , if a layer block from the local model does not match a corresponding global layer, we set  $\lambda_i = 0$ , meaning that the layer block will neither participate in the broadcasting nor aggregation processes. So the layers are participating according to their existing participation rate. For instance, if only 40% of clients have more than 4 layers, the generalization degree (in both broadcasting and aggregation stages), will be less than 0.4 in each training round due to different participation rates.

## 9. Theoretical Analysis

In this section, we provide the convergence analysis of  $pMixFed$ . Moreover, We compare the aggregation process and the server global model update of the  $FedSGD$  algorithm with our proposed mixed aggregation stage in  $pMixFed$ . We begin by introducing the key notations and assumptions used throughout the convergence analysis.

#### Notations:

- $t \in \{0, \dots, T-1\}$ : communication round index.
- $\eta_l$ : learning rate for local update,  $\eta_g$ : learning rate for global updates.
- $\lambda_{k,i}$ : mixup coefficient for client  $k$  at layer  $i$  in round  $t$ ,  $\lambda_k$ : mixup coefficient for client  $k$  in round  $t$  (assuming uniform across layers).
- $G^{(t)}$ : global model parameters at round  $t$ ,  $L_k^{(t)}$ : local model parameters of client  $k$  at round  $t$ .
- $|\mathcal{D}_k|$ : size of the dataset at client  $k$ ,  $|\mathcal{D}|$ : total size of datasets across all clients.
- $\nabla L_k^{(t+1)}$ : gradient of the local model at client  $k$  in round  $t$ .

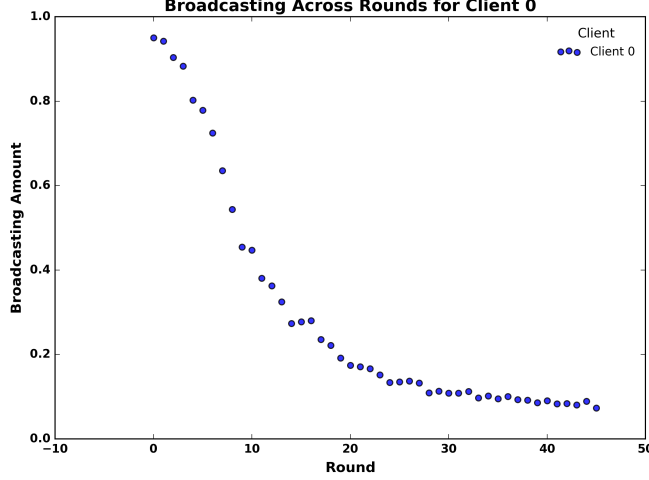


Figure 7. mix-factors for client 0 in different communication rounds

We make the following assumptions to establish the convergence properties of  $pMixFed$ :

**Assumption 1. Unbiased Gradient Estimation with Bounded Variance.** The gradient estimate for local model updates is unbiased and has a bounded variance, i.e.,

$$\mathbb{E}[\nabla \mathcal{L}_k^{(t)}] = \nabla \mathcal{L}_k^{(t)}, \quad \text{Var}(\nabla \mathcal{L}_k^{(t)}) \leq \sigma^2. \quad (9)$$

**Assumption 2 (Smoothness of Local Objectives).** The local objective functions  $L_k(\cdot)$  are  $L$ -smooth, i.e.,

$$\|\nabla L_k^{(t+1)} - \nabla L_k^{(t)}\| \leq L \|L_k^{(t+1)} - L_k^{(t)}\|. \quad (10)$$

**Assumption 3 (Bounded Gradients).** The gradients at each client are bounded, i.e.,

$$\|\nabla L_k^{(t+1)}\| \leq G, \quad \forall k, t. \quad (11)$$

These assumptions are standard in convergence analysis and ensure that the optimization process is well-behaved.

### 9.1. Local Training Convergence

We first analyze the local training updates that occur between communication rounds.

**Lemma 1. Local Model Training Progress.** Under Assumptions 2 and 1, after  $r$  local updates, the expected loss for client  $k$  satisfies:

$$\mathbb{E}[\mathcal{L}_k^{(t+r)}] \leq \mathcal{L}_k^{(t)} + \left( \frac{L_1 \eta_l^2}{2} - \eta_l \right) \sum_{j=0}^{r-1} \|\nabla \mathcal{L}_k^{(t+j)}\|^2 + \frac{L_1 r \eta_l^2 \sigma^2}{2}. \quad (12)$$

This lemma provides a bound on how the local training process improves the loss function. The bound depends on the learning rate  $\eta_l$ , the smoothness constant  $L_1$ , and the variance of the gradient estimates  $\sigma^2$ .

### 9.2. Global Model Aggregation

Next, we consider the effect of aggregating local models at the server after each communication round.

**Lemma 2. Global Model Aggregation Dynamics.** After aggregating the local models, the global model loss changes as follows:

$$\mathbb{E}[\mathcal{L}^{(t+1)}] \leq \mathbb{E}[\mathcal{L}^{(t)}] + \eta_g \delta^2, \quad (13)$$

where  $\delta^2$  bounds the difference between the global and local model parameters before and after aggregation.

This lemma shows that, during aggregation, the global loss increases by a term proportional to the global learning rate  $\eta_g$  and the parameter variation  $\delta^2$ .

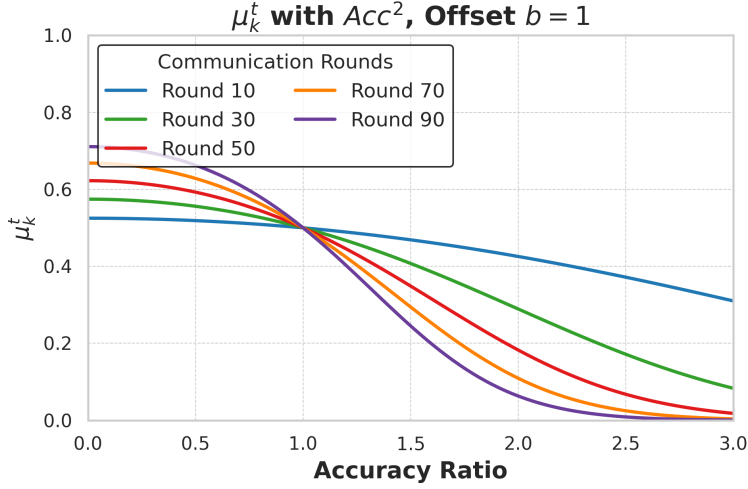


Figure 8. Adaptive mix-factor  $\mu_k^t$  according to the accuracy ratio  $Acc^t = Acc_L^t / Acc_G^t$  in different communication rounds.

### 9.3. Convergence of pMixFed

With the above lemmas, we can now derive the convergence properties of *pMixFed*.

**Theorem 1. Convergence Rate of pMixFed.** *Under the previously stated assumptions, the expected global loss after a complete round of communication and local training satisfies:*

$$\mathbb{E}[\mathcal{L}^{(t+1)}] \leq \mathcal{L}^{(t)} + \left( \frac{L_1 \eta_l^2}{2} - \eta_l \right) \sum_{k=1}^K \sum_{j=0}^{r-1} \|\nabla \mathcal{L}_k^{(t+j)}\|^2 + \frac{L_1 r \eta_l^2 \sigma^2}{2} + \eta_g \delta^2. \quad (14)$$

This theorem demonstrates that the global loss decreases with each communication round, with the convergence depending on the local and global learning rates, the gradient norms, and the parameter variation.

**Theorem 2. Non-Convex Convergence Rate.** *For non-convex loss functions, pMixFed achieves convergence at the following rate:*

$$\frac{1}{T} \sum_{t=0}^{T-1} \sum_{k=1}^K \|\nabla \mathcal{L}_k^{(t)}\|^2 \leq \mathcal{O}(1/T), \quad (15)$$

where  $T$  is the total number of communication rounds.

This final theorem indicates that *pMixFed* achieves non-convex convergence with a rate of  $\mathcal{O}(1/T)$ , demonstrating that the algorithm improves over time as the number of communication rounds increases.

### 9.4. The effect of Aggregating model parameters and gradients on catastrophic forgetting

In *FedSGD*, the gradients are aggregated and the server will be update the global model according to the aggregated gradients. the *FedSGD* is sometimes preferred over *FedAvg* due to its potentially faster convergence. However, it lacks robustness in heterogeneous environments. *pMixFed* leverages the faster convergence characteristics of *FedSGD* by incorporating early stopping mechanisms, facilitated by the use of mixup. As demonstrated in Section 5.4, the mixup factor  $\lambda$  functions analogously to an SGD update at the server, even though *pMixFed* aggregates model weights rather than gradients, similar to *FedAvg*. Section 9.4 provides a more detailed explanation of this mechanism.

the *pMixFed* algorithm combines the advantages of *FedSGD* and *FedAvg* by aggregating model weights rather than gradients, while still ensuring convergence even in heterogeneous data settings. The incorporation of the mixup mechanism enhances stability, providing faster convergence rates compared to *FedSGD*, particularly in non-convex settings. Considering local SGD steps  $r$  and  $\eta_l$  as the local learning rate we can further expand the above formulation:



$$\begin{aligned}
G^{t+1} &= G^t - \eta_g \sum_{i=1}^k \Omega_k \left[ L_k^{(t+r)} - L_k^{(t)} \right] \\
G^{t+1} &= G^t - \eta_g \cdot \eta_l \sum_{i=1}^k \Omega_k \sum_{j=0}^{r-1} \nabla L_k^{(t+j)}
\end{aligned} \tag{16}$$

Since in FedSGD, the global model  $G^{(t)}$  is fully shared with each local model  $L_k^{(t)}$  in each communication round  $t$ , and  $\sum_{i=1}^k \Omega_k = 1$ , we can update the problem as a constrained optimization problem.

$$\begin{aligned}
G^{t+1} &= G^t - \eta_g \cdot \eta_l \sum_{j=1}^{r-1} \nabla G^{(t+j)} \\
\sum_{j=2}^{r-1} \nabla G^{(t+j)} &= (1 - \eta_g \cdot \eta_l) G^t - (1 + \eta_g \cdot \eta_l) G^{t+1}
\end{aligned}$$

The right term of the equation is the history of global model gradients which could be written as  $H \Big|_2^{r-1} \nabla G^t = a \cdot G^t - b \cdot G^{t+1}$ . The problem of the FedSGD algorithm is that the gradients are too small to keep the state of the previous global model, leading to catastrophic forgetting in partial models that use gradients in their aggregation stage. We hypothesize that the mixup coefficient  $\lambda$  acts similarly to the learning rate  $\eta$ , suggesting that  $\lambda$  plays a role analogous to  $\eta$  in *FedSGD*.

**FedSGD Update Rule :** In *FedSGD*, the global model  $G^{(t)}$  is updated by aggregating the gradients from all clients:

$$G^{(t+1)} = G^{(t)} - \eta_g \sum_{k=1}^K \Omega_k \nabla L_k^{(t+1)}, \tag{17}$$

where  $\Omega_k = \frac{|D_k|}{|D|}$  is the weight associated with client  $k$ . Since  $L_k^{(t+1)} = L_k^{(t)} - \eta_l \nabla L_k^{(t+1)}$ , we can rewrite the update as:

$$G^{(t+1)} = G^{(t)} - \eta_g \sum_{k=1}^K \Omega_k \left( \frac{L_k^{(t)} - L_k^{(t+1)}}{\eta_l} \right). \tag{18}$$

**pMixFed Update Rule:** In *pMixFed*, the global model update incorporates mixup coefficients:

$$G^{(t+1)} = \sum_{k=1}^K \Omega_k \left[ (1 - \lambda_k) L_k^{(t+1)} + \lambda_k G^{(t)} \right]. \tag{19}$$

Assuming  $\lambda_{k,i} = \lambda_k$  for all layers  $i$ , and considering that  $G^{(t)}$  is sent to all clients at round  $t$ , we simplify the update to:

$$G^{(t+1)} = (1 - \lambda_k) \sum_{k=1}^K \Omega_k L_k^{(t+1)} + \lambda_k G^{(t)}. \tag{20}$$

#### 9.4.1. Analytical analysis of the Effect of learning rate and mixup degree

To establish the relationship between  $\lambda$  and  $\eta_g$ , we align the *FedSGD* and *pMixFed* update equations. From Equation (20), rearranged:

$$G^{(t+1)} - \lambda_k G^{(t)} = (1 - \lambda_k) \sum_{k=1}^K \Omega_k L_k^{(t+1)}. \tag{21}$$

From Equation (18), rearranged:

$$G^{(t+1)} = G^{(t)} - \frac{\eta_g}{\eta_l} \sum_{k=1}^K \Omega_k \left( L_k^{(t)} - L_k^{(t+1)} \right). \tag{22}$$

Assuming  $L_k^{(t)}$  is replaced with  $G^{(t)}$  at round  $t$  for *FedSGD*, we have  $L_k^{(t)} = G^{(t)}$ . Substituting this into Equation (22):

$$G^{(t+1)} = G^{(t)} - \frac{\eta_g}{\eta_l} \sum_{k=1}^K \Omega_k \left( G^{(t)} - L_k^{(t+1)} \right). \tag{23}$$

Simplifying and Comparing with Equation (20), we see that if:  $\lambda_k = \frac{\eta_g}{\eta_l}$ , then the updates are analogous.

$$G^{(t+1)} = G^{(t)} \left( 1 - \frac{\eta_g}{\eta_l} \sum_{k=1}^K \Omega_k \right) + \frac{\eta_g}{\eta_l} \sum_{k=1}^K \Omega_k L_k^{(t+1)}. \tag{24}$$

**Theorem 3.** Under Assumptions 2 and 3, the mixup coefficient  $\lambda_k$  in *pMixFed* acts similarly to the learning rate ratio  $\frac{\eta_g}{\eta_l}$  in *FedSGD*, such that:  $\lambda_k = \frac{\eta_g}{\eta_l}$ . This implies that the mixup mechanism in *pMixFed* can be interpreted as a form of learning rate control analogous to *FedSGD*.

*Proof.* Starting from the *pMixFed* update in Equation (21):

$$G^{(t+1)} - \lambda_k G^{(t)} = (1 - \lambda_k) \sum_{k=1}^K \Omega_k L_k^{(t+1)}. \quad (25)$$

From the rearranged *FedSGD* update in Equation (24):

$$G^{(t+1)} = G^{(t)} \left(1 - \frac{\eta_g}{\eta_l}\right) + \frac{\eta_g}{\eta_l} \sum_{k=1}^K \Omega_k L_k^{(t+1)}. \quad (26)$$

Setting the two expressions equal:

$$\begin{aligned} G^{(t)} (1 - \lambda_k) + (1 - \lambda_k) \sum_{k=1}^K \Omega_k L_k^{(t+1)} = \\ G^{(t)} \left(1 - \frac{\eta_g}{\eta_l}\right) + \frac{\eta_g}{\eta_l} \sum_{k=1}^K \Omega_k L_k^{(t+1)}. \end{aligned} \quad (27)$$

This simplifies to:

$$\lambda_k = \frac{\eta_g}{\eta_l}. \quad (28)$$

Given that  $\lambda_k$  must lie in the range  $[0, 1]$ , this relationship holds when  $\eta_g \leq \eta_l$ . Since both  $\eta_g$  and  $\eta_l$  are also constrained within the interval  $[0, 1]$ , our findings are consistent with previous studies [10, 33], which recommend keeping the head unfrozen (i.e.,  $\eta_l \neq 0$ ). □

**Remark1.** Theorem 3 establishes a direct relationship between the mixup coefficient  $\lambda_k$  and the learning rates used in local and global updates. This insight allows us to interpret the mixup mechanism in *pMixFed* as adjusting the effective learning rate at the server, providing a theoretical foundation for selecting  $\lambda_k$  based on desired convergence properties.

**Remark2.** In practice, this relationship suggests that by tuning  $\lambda_k$ , we can control the influence of the global model versus the local models in the aggregation process, similar to adjusting the learning rate in *FedSGD*. This is particularly beneficial in heterogeneous environments where clients may have varying data distributions.

Our theoretical analysis indicates that the mixup coefficient  $\lambda_k$  in *pMixFed* plays a role analogous to the learning rate in *FedSGD*. This equivalence provides a deeper understanding of how *pMixFed* leverages the strengths of *FedSGD* while mitigating its weaknesses in heterogeneous settings. By appropriately choosing  $\lambda_k$ , *pMixFed* can achieve faster convergence and improved robustness.

## 10. Additional Details about the Experiments

### 10.1. Experimental Setup

**Dataset:** We used three widely used federated learning datasets: **MNIST** [23], **CIFAR-10**, **CIFAR-100** [3], and **EMNIST** [8]. CIFAR-10 consists of 50,000 images of size  $32 \times 32$  for training and 10,000 images for testing. CIFAR-100, on the other hand, consists of 100 classes, with 500  $32 \times 32$  images per class for training and 100 images per class for testing. MNIST contains 10 labels and includes 60,000 samples of  $28 \times 28$  grayscale images for training and 10,000 for testing. For creating heterogeneity, we followed the

**Training Details:** For evaluation, We have reported the average test accuracy of the global model [59] for different approaches. The final global model at the last communication round is saved and used during the evaluation. The global model

is then personalized according to each baseline’s personalization or fine-tuning algorithm for  $r = 4$  local epochs and  $T = 50$ . For **FedAlt**, the local model is reconstructed from the global model and fine-tuned on the test data. For **FedSim**, both the global and local models are fine-tuned partially but simultaneously. In the case of **FedBABU**, the head (fully connected layers) remains frozen during local training, while the body is updated. Since we could not directly apply **pFedHN** in our platform setting, we adapted their method using the same hyper parameters discussed above and employed hidden layers with 100 units for the hypernetwork and 16 kernels. The local update process for **LG-FedAvg**, **FedAvg**, and **Per-FedAvg** simply involves updating all layers jointly during the fine-tuning process. The global learning rate for the methods that need sgd update in the global server e.g., FedAvg, has been set from  $lr_{global} = [1e - 3, 1e - 4, \text{and} 1e - 5]$ . It should be noted that due to the performance drop for some methods (FedAlt , FedSim) in round 10 or 40 in some settings, we’ve reported the highest accuracy achieved. Also this is the reason the accuracy curves are illustrated for 39 rounds instead of 50. <sup>5</sup>

## 10.2. Out-of-Sample and Participation Gap

In the evaluation of the effect of learning rate and mixup, the average test accuracy<sup>6</sup> is measured on cold-start clients  $|D_{k \cap \text{unseen}}^{ts}|, k \in \{1, \dots, M\}$ , where  $D^{ts} \neq D^{tr}$ . These clients have not participated in the federation at any point during training. FedAlt and FedSim perform poorly on cold-start users or unseen clients, highlighting their limited generalization capability. The test accuracy of pFedMix, while affected under a 10% participation rate, benefits significantly from seeing more clients. Increased client participation directly improves accuracy, as observed in previous studies [34].

## 10.3. Ablation Study : The Effects of Different alpha on Mixup Degree

The Beta distribution  $\beta(\alpha, \alpha)$  is defined on the interval [0,1], where the parameter  $\alpha$  controls the shape of the distribution. The value of  $\lambda$ , used in Eq. 4, is naturally sampled from this distribution. By varying the parameter  $\alpha$ , we can adjust how much mixing occurs between the global model  $G$  and the local model  $L_k$ .

- **Uniform Distribution:** When  $\alpha = 1$ , the Beta distribution becomes uniform over [0,1]. In this case,  $\lambda$  is sampled uniformly across the entire interval, meaning that each model,  $G$  and  $L_k$ , has an equal probability of being weighted more or less in the mixup process. This leads to a broad exploration of different combinations of global and local models, allowing for a wide range of mixed models.
- **Concentrated Mixup ( $\alpha > 1$ ):** When  $\alpha > 1$ , the Beta distribution is concentrated around the center of the interval [0,1]. As a result, the mixup factor  $\lambda$  is more likely to be closer to 0.5, leading to more balanced combinations of the global and local models. This results in outputs that are more "mixed," with neither model dominating the mixup process. Such a setup can enhance the robustness of the combined model, as it prevents extreme weighting of either model, creating smoother interpolations between them.
- **Extremal Mixup ( $\alpha < 1$ ):** In contrast, when  $\alpha < 1$ , the Beta distribution becomes U-shaped, with more probability mass near 0 and 1. This means that  $\lambda$  tends to be either very close to 0 or very close to 1, favoring one model over the other in the mixup process. When  $\lambda \approx 0$ , the local model  $L_k$  is chosen almost exclusively, and when  $\lambda \approx 1$ , the global model  $G$  is predominantly selected. This form of mixup creates a more deterministic selection between global and local models, with less mixing occurring.

The behavior of different  $\alpha$  values is depicted in Figure 9, where the distribution of the mixup factor  $\lambda$  is visualized. These distributions highlight the varying degrees of mixup, ranging from uniform blending to nearly deterministic model selection. To thoroughly investigate the impact of  $\alpha$  on model performance, we designed two distinct experimental setups:

- **Random Sampling:** In this scenario, we set different  $\alpha$ , meaning that the  $\lambda$  values are sampled uniformly from the interval [0,1] according. This ensures a wide range of mixup combinations between the global and local models. The random sampling approach helps us assess the general robustness of the model when the mixup degree  $\lambda$  is not biased towards any specific value. Table 3 shows the effect of different  $\alpha$  on the overall test accuracy of pMixFed.
- **Adaptive Sampling:** For this case, we divided the communication rounds into three distinct stages, each consisting of  $\frac{\text{epoch}_{global}}{3}$  epochs. During these stages, the parameter  $\alpha$  is adaptively changed as follows:

$$\alpha = \begin{cases} 0.1, & \text{initial stage (early training)} \\ 100, & \text{middle stage (convergence phase)} \\ 10, & \text{final stage (fine-tuning)} \end{cases} \quad (29)$$

<sup>5</sup>As discussed in the main paper, the change of hyper-parameters such as lr, batch size, momentum and even changing the optimizer to adam didn’t help with the performance drop in most cases.

<sup>6</sup>Classification accuracy using softmax

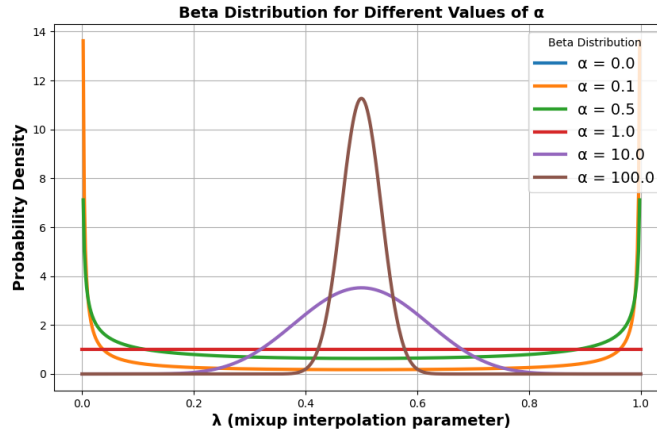


Figure 9. PDF  $\lambda$  (mixup degree) for different values of  $\alpha$  in  $\beta$  distribution

This adaptive strategy mimics the behavior of the original pFedMix algorithm while also allowing for more controlled exploration of different mixup combinations. During the early and late stages, a small  $\alpha$  (0.1) encourages more deterministic model selections (i.e., either local or global), while the middle stage with  $\alpha = 100$  promotes more balanced mixing. This dynamic adjustment of  $\alpha$  enables us to control the degree of mixup at different phases of training. Table 4 also shows the effect of different sampling approaches (random and adaptive) on the overall test accuracy of all three dataset *pMixFed*. The results shows that the adaptive sampling which creates a form scheduling for mixup degree shows promising result even compared to the original algorithm using adaptive  $\mu$ .

Table 3. Accuracy of *pMixFed* with Different  $\alpha$  Values in the Beta Distribution

Dataset	$\alpha = 0.1$	$\alpha = 0.5$	$\alpha = 1$	$\alpha = 2$	$\alpha = 5$
CIFAR-10	78.5	81.2	82.6	84.3	83.1
CIFAR-100	42.3	45.6	47.2	49.8	48.1

Table 4. Accuracy of *pMixFed* with Different  $\alpha$  Values and Sampling Strategies

Dataset	Sampling Strategy	Accuracy(%)
CIFAR-10	Random Sampling ( $\alpha = 1$ )	82.6
CIFAR-10	Adaptive Sampling	85.3
CIFAR-100	Random Sampling ( $\alpha = 1$ )	47.2
CIFAR-100	Adaptive Sampling	50.1
MNIST	Random Sampling ( $\alpha = 1$ )	97.9
MNIST	Adaptive Sampling	98.6